AFRL-PR-WP-TP-2006-268

HYDROXYL TAGGING VELOCIMETRY IN CAVITY-PILOTED MACH 2 COMBUSTOR (POSTPRINT)

M.D. Lahr, R.W. Pitz, Z.W. Douglas, and C.D. Carter

OCTOBER 2006

STINFO COPY

**PROPULSION DIRECTORATE
AIR FORCE MATERIEL COMMAND
AIR FORCE RESEARCH LABORATORY
WRIGHT-PATTERSON AIR FORCE BASE, OH 45433-7251**

REPORT DOCUMENTATION PAGE

*Form Approved
OMB No. 0704-0188*

The public reporting burden for this collection of information is estimated to average 1 hour per response, including the time for reviewing instructions, searching existing data sources, searching existing data sources, gathering and maintaining the data needed, and completing and reviewing the collection of information. Send comments regarding this burden estimate or any other aspect of this collection of information, including suggestions for reducing this burden, to Department of Defense, Washington Headquarters Services, Directorate for Information Operations and Reports (0704-0188), 1215 Jefferson Davis Highway, Suite 1204, Arlington, VA 22202-4302. Respondents should be aware that notwithstanding any other provision of law, no person shall be subject to any penalty for failing to comply with a collection of information if it does not display a currently valid OMB control number. **PLEASE DO NOT RETURN YOUR FORM TO THE ABOVE ADDRESS.**

1. REPORT DATE *(DD-MM-YY)*	2. REPORT TYPE	3. DATES COVERED *(From - To)*
October 2006	Conference Paper Postprint	N/A

4. TITLE AND SUBTITLE

HYDROXYL TAGGING VELOCIMETRY IN CAVITY-PILOTED MACH 2 COMBUSTOR (POSTPRINT)

5a. CONTRACT NUMBER
In-house

5b. GRANT NUMBER

5c. PROGRAM ELEMENT NUMBER
61102F

6. AUTHOR(S)

M.D. Lahr, R.W. Pitz, and Z.W. Douglas (Vanderbilt University)
C.D. Carter (AFRL/PRAS)

5d. PROJECT NUMBER
2308

5e. TASK NUMBER
AI

5f. WORK UNIT NUMBER
00

7. PERFORMING ORGANIZATION NAME(S) AND ADDRESS(ES)

Vanderbilt University
Department of Mechanical
 Engineering
Nashville, TN 37235

Propulsion Sciences Branch (AFRL/PRAS)
Aerospace Propulsion Division
Propulsion Directorate
Air Force Research Laboratory, Air Force Materiel Command
Wright-Patterson AFB, OH 45433-7251

8. PERFORMING ORGANIZATION REPORT NUMBER

AFRL-PR-WP-TP-2006-268

9. SPONSORING/MONITORING AGENCY NAME(S) AND ADDRESS(ES)

Propulsion Directorate
Air Force Research Laboratory
Air Force Materiel Command
Wright-Patterson AFB, OH 45433-7251

10. SPONSORING/MONITORING AGENCY ACRONYM(S)
AFRL-PR-WP

11. SPONSORING/MONITORING AGENCY REPORT NUMBER(S)
AFRL-PR-WP-TP-2006-268

12. DISTRIBUTION/AVAILABILITY STATEMENT
Approved for public release; distribution is unlimited.

13. SUPPLEMENTARY NOTES
Conference paper published in the Proceedings of the 2006 44th AIAA Aerospace Sciences Meeting and Exhibit, published by AIAA.

© 2006 Michael Lahr. The U.S. Government is joint author of the work and has the right to use, modify, reproduce, release, perform, display, or disclose the work. PAO case number: AFRL/WS 06-0004; Date cleared: 03 Jan 2006. Paper contains color.

14. ABSTRACT
Hydroxyl tagging velocimetry (HTV) measurements of velocity were made in a Mach 2 scramjet combustor with a wall cavity flameholder. In the HTV method, ArF excimer laser (193 nm) beams pass through a humid gas flow and dissociate H_2O into H + OH to form a tagging grid of OH molecules. Previously demonstrated with a 7x7 grid of hydroxyl (OH) molecules, HTV is now demonstrated with an 11x11 grid of OH tracked by planar laser-induced fluorescence to yield about 120 velocity vectors of the two-dimensional flow over a fixed time delay. Instantaneous, single-shot measurements of two-dimensional flow patterns were made in the non-reacting Mach 2 flow from step to step in the cavity under low- and high-backpressure conditions. Single-shot profiles were analyzed to yield mean and rms velocity profiles in the Mach 2 non-reacting flow. A set of velocity data (spanning the entire length of the cavity) for an open wall cavity in a supersonic flow under low and high backpressure conditions was compiled for validation of CFD models.

15. SUBJECT TERMS

16. SECURITY CLASSIFICATION OF:			17. LIMITATION OF ABSTRACT:	18. NUMBER OF PAGES	19a. NAME OF RESPONSIBLE PERSON (Monitor)
a. REPORT Unclassified	**b. ABSTRACT** Unclassified	**c. THIS PAGE** Unclassified	SAR	22	Campbell D. Carter **19b. TELEPHONE NUMBER** *(Include Area Code)* N/A

Standard Form 298 (Rev. 8-98)
Prescribed by ANSI Std. Z39-18

i

Hydroxyl Tagging Velocimetry in Cavity-Piloted Mach 2 Combustor

M. D. Lahr[*], R. W. Pitz[†], Z. W. Douglas[‡]
Department of Mechanical Engineering, Vanderbilt University, Nashville, Tennessee 37235

C. D. Carter[§]
Air Force Research Laboratory (AFRL/PRAS), Wright-Patterson Air Force Base, Ohio 45433

Hydroxyl tagging velocimetry (HTV) measurements of velocity were made in a Mach 2 scramjet combustor with a wall cavity flameholder. In the HTV method, ArF excimer laser (193 nm) beams pass through a humid gas flow and dissociate H_2O into H + OH to form a tagging grid of OH molecules. Previously demonstrated with a 7x7 grid of hydroxyl (OH) molecules, HTV is now demonstrated with an 11x11 grid of OH tracked by planar laser-induced fluorescence to yield about 120 velocity vectors of the two-dimensional flow over a fixed time delay. Instantaneous, single-shot measurements of two-dimensional flow patterns were made in the non-reacting Mach 2 flow from step to step in the cavity under low- and high-backpressure conditions. Single-shot profiles were analyzed to yield mean and rms velocity profiles in the Mach 2 non-reacting flow. A set of velocity data (spanning the entire length of the cavity) for an open wall cavity in a supersonic flow under low and high backpressure conditions was compiled for validation of CFD models.

I. Introduction

Realistic and accurate velocimetry measurements are essential to the advancement of supersonic and hypersonic capabilities. In scramjet vehicles, wall cavities are commonly used to stabilize the core-flow flame without excessive drag penalty. They also provide a recirculation region with sufficient residence time for a sustaining reaction and core-flow mass exchange. Velocity measurements are needed in this type of configuration under supersonic conditions for modeling and simulation purposes but require non-intrusive methods, where probes can easily produce flow disturbances. Typically, non-intrusive gas-phase velocity measurements are made with laser scattering from particles either inserted or naturally available in the flow. These techniques include particle image velocimetry, laser Doppler velocimetry, planar Doppler velocimetry, and phase Doppler anemometry.[1,2] The use of particles in laser velocimetry requires the particles to follow the fluid streamlines of the corresponding unseeded flow. However, in supersonic flows the particle velocity often differs from the actual gas velocity due to particle drag and a slow response to velocity gradients.[3] Also, particle seeding in a confined flow can cause window coating, limiting test times and possibly causing window abrasion. The flow rate and areas in the test section available for measurements can also be affected.[4]

Laser-based molecular velocity methods directly measure the gas velocity in the flow, negating the various problems posed by particle-based methods. Typical molecular-based methods include Doppler-shift techniques and molecular tagging. In Doppler-shift methods, the Doppler shift of molecules (or atoms) that are added to the flow are measured and related to velocity. These methods are based on laser-induced fluorescence of the molecules (or atoms) inserted in the flow such as copper[5], hydroxyl[6,7], nitric oxide[8], sodium[9], and iodine[10]. Doppler-shift methods are better suited for higher velocity environments where the Doppler shift is much larger and more easily measured. However, they often yield only average flow velocities due to a lack of signal strength. Although there has been success with the use of Doppler-based molecular velocimetry methods, the addition of chemical species is often

---

[*] Graduate Student, Mechanical Engineering Department, Nashville, TN 37235-1592, Student member

[†] Professor, Department of Mechanical Engineering, Nashville, TN 37235-1592, AIAA Associate Fellow

[‡] Undergraduate Student, Mechanical Engineering Department, Nashville, TN 37235-1592, Non-member

[§] Senior Aerospace Engineer, Aerospace Propulsion Division (AFRL/PRA), 1950 Fifth St., Wright-Patterson Air Force Base, OH 45433, AIAA Associate Fellow

1
American Institute of Aeronautics and Astronautics

impractical in test facilities. Seeding a large facility can become very expensive. It also may pose a risk for high levels of toxicity and corrosive behavior, and many of these seeded molecules exhibit thermal decomposition at higher temperatures. In Doppler-shift methods the optical geometry of the laser and the observer define the velocity component that is measured, and this feature can be limiting. Many laser-induced fluorescence methods that make use of the Doppler-shift can only be used to measure the component of the velocity in the direction of propagation of the laser sheet.[11] Other Doppler-shift velocity methods are based on Rayleigh scattering from the gas molecules.[12,13] Rayleigh scattering signals are typically weaker and harder to obtain in confined facilities than those produced by Doppler fluorescence owing to the interference caused by laser scattering from the walls and particles in the flow.[11]

Other laser-based molecular velocity methods are based on molecular tagging. Molecular tagging techniques yield the gas velocity by time of flight; the molecules in the gas flow are tagged or marked with a laser, and the movement of the tag gives the velocity. Once a laser line or grid is tagged, the grid will move with the flow. There is no particle drag or non-uniformity issues associated with molecular velocimetry.The movement of the tagged regions is imaged by a method dictated by the photochemistry of the tagged molecules (laser-induced fluorescence in the case of hydroxyl tagging velocimetry). The displacement of the tagged grid over a fixed time period yields the velocity. This time-of-flight measurement of velocity can be easily implemented because it does not require the complex calibrations or corrections necessary in the Doppler shift method. Some molecular tagging methods, similar to Doppler-based molecular velocity methods, use a gas seed. A gas molecule (or atom) is added to the flow and the molecule is tagged with a laser beam. The molecule can, for example, be electronically excited, photodissociated, or vibrationally excited. Researchers have used a variety of molecular tags in this technique including acetone,[14] biacetyl,[15,16] nitric oxide,[11,17] nitrogen dioxide,[18] sodium,[19] strontium[20] and *tert*-butyl nitrate.[21] Again, seeding a flow with molecules or atoms is often undesirable due to a variety of reasons (expense, seeding toxicity, corrosive behavior, thermal decomposition, etc.).

"Unseeded" molecular tagging methods use gas tags produced from molecules naturally occurring in air (i.e., nitrogen, oxygen, water vapor). They include N_2^+ ion[22], ozone[23-25], hydroxyl[25-30], nitric oxide[31-33], and vibrationally excited oxygen.[13,34] Many of the methods use non-linear laser excitation[13,22,26,31-34] to produce these tags from air and the tag is only produced in a small region near the laser focus. In this work, the "unseeded" hydroxyl based molecular tagging method is used. Hydroxyl tagging velocimetry is a linear method[28-30] in which an ArF laser, operating at 193 nm wavelength, photodissociates water in a humid flow. In this single-photon process, photodissociation of vibrationally excited H_2O creates lines of OH at a concentration higher than the ambient OH. The OH grid moves for a known period of time and is recorded with laser-induced fluorescence. Hydroxyl is an optimal tag for this supersonic application as OH is formed immediately by the pulsed laser through H_2O photodissociation, and OH has an adequate lifetime in the supersonic flow. Also, the use of hydroxyl allows for long lines to be written in a hot flow associated with a scramjet, creating more flexibility and accessibility in the test area setup.

Non-intrusive velocity data is needed in flows relevant to scramjet combustion. An optically accessible supersonic flow facility has been developed to study cavity-stabilized supersonic reacting flows. Velocity data from this study can be used as a comparison or parameter for advanced computational fluid dynamics models.[36-38] The HTV method is applied to a Mach 2 flow with a wall cavity flame holder to obtain instantaneous two-dimensional velocity images, mean velocity profiles, and rms velocity profiles. Velocity measurements are made by using HTV in the freestream and within the cavity of the Mach 2 cavity-piloted combustor.

II. Experimental System

The hydroxyl tagging velocimetry experiments were conducted at the supersonic flow facility in Research Cell 19 at the Air Force Research Laboratory in the Propulsion Directorate at Wright-Patterson Air Force Base. A schematic of the flow facility is shown in Figure 1. The air supply to the wind tunnel consists of a series of compressors and a gas-fired heat exchanger to produce high-pressure/high-temperature air at the desired test conditions. A uniform, two-dimensional, Mach 2 stream exiting from the nozzle is present at the entrance to the test section with the flow symmetric about the transverse and spanwise centerlines. Past the nozzle, there is a constant-area section, upstream of a flame holder cavity, with a cross section of 51 mm high by 153 mm wide. Downstream of the constant-area section, in the test section, the bottom wall diverges at an angle of 2.5°. A cavity to provide a flame pilot forms the bottom surface of the tunnel. Fig. 2 shows a schematic of the cavity (the flow is left to right). It is 17 mm deep and 66 mm long. A shear layer forms at the edge of the first step in the cavity, and the recirculation zone is produced by the cavity.

American Institute of Aeronautics and Astronautics

The HTV measurements were taken in the flame holder cavity of the combustor test section. A schematic of the HTV system is shown in Fig. 3. Air entered the test section at Mach 2 with a flowrate of approximately 1.4 kg/s. A Lambda Physik Compex 150T ArF excimer laser was used to produce a 193 nm laser beam. The ArF excimer laser setup had to be configured to achieve accessible angles through the windows to create the greatest number of visible crossing points and the least amount of laser scattering. Three different configurations were used to proceed downstream of the leading edge of the cavity, however; only the position of the grid optics had to be altered to allow for accessible measurements. The basis for the setup, as shown in Fig. 3, consists of the ArF excimer laser beam (20 mm high by 10 mm wide, 150 mJ/pulse, broadband, 1 nm bandwidth) being split into two beams by a beam splitter, one traveling under the test section to the other side, and the other beam remaining on the same side of the configuration. This provided adequate crossing angles for the written lines in the flow regime across the cavity. The laser grids come in from both sides of the test section with the camera mounted above the tunnel. Each of the laser beams is sent through the new grid-forming optics to produce two sets of eleven beams each. The grid optics consist of two major components placed very close together: a 300 mm focal length cylindrical lens (25 mm x 40 mm) and a stack of eleven cylindrical lenses (20 mm wide by 2 mm high). The beam diameter was about 0.3 mm in the measurement zone. The energies for the two sets of beams before transmission into the tunnel were measured at as low as 9.4 mJ/pulse on the excimer laser side with a path length of 2.79 m and 7.4 mJ/pulse on the dye laser side with a path length of 3.91 m.

The ArF excimer generated an 11 x 11 grid of OH "lines" that was subsequently imaged by laser-induced fluorescence using the overlapped $Q_1(1) + R_2(3)$ transition of the $A^2\Sigma^+$ ($v' = 1$) $\leftarrow X^2\Pi_i$ ($v'' = 0$) band at 282 nm. A Spectra Physics Model GRC 170 Nd:YAG laser (injection seeded) pumped a Lumonics HD-300 Hyperdye dye laser. The output of the dye laser was doubled by an Inrad Autotracker II to produce about 20 mJ/pulse of 282 nm laser radiation. A small portion of the 282 nm beam was split off and directed over a small flame and then to a photodiode. Signals from the photodiode and a photomultiplier tube—recording the OH laser-induced fluorescence from the flame—were displayed on an oscilloscope to ensure proper operation of the dye laser and good overlap with the OH transition. Timing of the lasers and camera was accomplished with a Quantum Composer (Model 9318E) pulse generator. Random (shot-to-shot) timing error between the lasers was about ±20 ns or about ±1% of the typical 2 μs timing separation.

The 282-nm beam was expanded by a -150 mm focal length cylindrical lens and focused by a 1000 mm focal length spherical lens to form a sheet. Retro-reflection of the laser sheet back through the tunnel was implemented to improve signal strength. The delay was about 5 ns. Both the OH-probe laser sheet and the 193 nm grid were rotated parallel to the tunnel bottom floor at an angle of 2.5° off the horizontal plane.

A PIMAX "Superblue" intensified CCD camera was used to record the fluorescence from the created OH. The camera was fitted with a 45-mm f/1.8 UV Cerco lens and Schott glass filters (WG-305 and UG-5) were employed to block background scattering and fluorescence from tunnel surfaces. With the camera looking down through the top window of the test section, the field of view was 40 mm square. The 512 x 512 pixel array of the PIMAX camera was binned 2 x 2 to improve signal strength, with each 2 x 2 binned pixel having dimensions of 156 μm x 156 μm.

A three-dimensional traversing table was located beneath the tunnel. Focusing optics for the setup and the ICCD camera were arranged and mounted on the table to allow the laser grid and sheet height location to be varied. The velocity trends above and down into the cavity could then be probed.

III. Results

HTV measurements were made in non-reacting Mach 2 flow with an 11 x 11 grid pattern. The conditions for the experiments are shown in Table 1. Test A is a low-backpressure condition with the backpressure valve fully open downstream of the test section. Test B is a high-backpressure condition with the backpressure valve 60% closed to simulate the pressure rise from main-duct combustion. The two tests were conducted to explore the velocity trends in the test section with and without shock waves present in the cavity flow. Under low backpressure conditions, the tunnel flow above the cavity is basically free of shock waves with only a few weak oblique shocks anchored to the leading edge as shown in Fig. 4.[39] With the backpressure valve partly closed, creating high-backpressure, strong shocks appear above the cavity causing the shear layer to be deflected upward (see Fig. 2 of Ref. 38).

Dry air from the compressors used to run the wind tunnel did not contain adequate humidity levels to achieve strong OH signals for hydroxyl tagging velocimetry. Water was sprayed into the stagnation chamber to provide moist air. Water flowrates varied from 17 g/s to 25 g/s with the relative humidity reaching up to 32% to improve the OH signal with no condensation or water droplets forming on the windows or in the flow. HTV measurements were

made along the streamwise length of the cavity with measurements taken vertically at each location. The regions analyzed can be seen in Fig. 5 with the distinction of the measurement zone. The position of the OH grid regions with respect the cavity walls are shown. Examples of two-dimensional velocity images utilizing the HTV method with the 11 x 11 grid are shown in Figs. 6, 7, 8, and 9. Fig. 6 is an averaged HTV image (100 single-shots) used as a reference for the displaced grid patterns. Figs. 7, 8, and 9 are analyzed HTV images with velocity vectors shown on top of displaced 11 x 11 HTV grid patterns. The method used to obtain the vector field was also used previously with the 7 x 7 grid pattern[40] with the details of the procedure described by Gendrich and Koochesfahani.[41] Figs. 7, 8, and 9 include both irregular grid and regular grid spacing for the vector representation. The irregular grid pattern from the HTV images shown on the left is mapped onto a regular grid shown on the right. The details of the procedure and its performance characteristics are given by Cohn and Koochesfahani.[42] The time delays varied in these experiments from 1 μs to 3 μs with the delay at 2 μs for all freestream measurements.

In the freestream above the cavity shown in Fig. 7, the velocity pattern is very uniform with a value of about 680 m/s (note the reference vector of 700 m/s) with the higher velocity (higher than expected for the Mach 2 nozzle) due to the bottom wall divergence. Moving down into the shear layer, the flow becomes much less uniform and exhibits a decrease in velocity to about 175 m/s (note reference vector of 300 m/s) as seen in Fig. 8. A single-shot image of flow in the cavity is shown in Fig. 9. At this depth the flow reverses with the negative velocity reaching up to 200 m/s (note reference vector of 200 m/s).

The average signal-to-noise ratio of the single-shot images is about 5-11. With crossing angles between 135° and 150°, the center of the line crossings can be determined within 0.1 pixels or a displacement uncertainty of $\pm$ 16 μm according to previous calculations (see Fig. 5 of Ref. 41). The uncertainty due to the characteristics of the crossing points is therefore about 5 m/s for a 3 μs delay, 8 m/s for a 2 μs delay, and 16 m/s for a 1 μs delay. Thus, for full-scale displacement, as seen in the freestream, a relative uncertainty of about $\pm$ 1% can be achieved.

Mean velocity and rms velocity profiles were obtained by analyzing instantaneous velocity images (100 single-shots at each data point) at various streamwise locations (x-axis) in the cavity shown in Fig. 10. Streamwise velocity profiles are shown near the centerline of the tunnel from the freestream to down in the cavity in Fig. 11. The average velocities above the cavity range from about 680 m/s to 730 m/s. The velocity in the freestream is higher at the inlet to the cavity (x = 0) due to the velocity drop that occurs across the oblique shock anchored to the leading edge as seen in Fig. 4.[39] The average velocity decreases in the shear layer and becomes negative (about -75 m/s) in the cavity. The shear layer profile appears typical of flows formed behind a rearward-facing step.[43] The shear layer width grows with downstream distance, as expected.

The rms velocities for the low-backpressure case are shown in Fig. 12. The rms values in the freestream are as low as 8 m/s, or about 1.2%. This rms value is due to a combination of freestream turbulence and measurement precision. Recall that the displacement error is about $\pm$ 1% and the timing error is about $\pm$ 1% (statistics on the timing jitter were not performed) of the typical 2 μs delay; of course, the timing error could be largely eliminated by recording the timing for each image with a photodiode. The rms values increase in the shear layer and then decrease slightly in the cavity similar to what is observed in the flow behind a rearward-facing step.[43]

The mean and rms values for the high-backpressure case are shown in Figs. 13 and 14. The profiles are quite different than those for the low-backpressure case. Shock waves observed previously[38] greatly alter the mean and rms values of the velocity. The mean velocities are slightly lower with the presence of shocks. The profiles do not correspond to those seen in subsonic flows behind a rearward-facing step.[43] In this unsteady compressible flow with shocks, the shear layer is deflected upward.[38] Therefore the rms values are highest above the cavity, where shocks have been previously observed (see Fig. 2 of Ref. 38).

IV. Conclusions

Previously demonstrated with a 7x7 grid pattern, non-intrusive measurements of velocity were obtained in a Mach 2 flow with a wall cavity flameholder using hydroxyl tagging velocimetry in one centralized location. With an 11 x 11 grid pattern to display a greater number of vectors in the flow field, velocity measurements are obtained from edge-to-edge in the Mach 2 non-reacting flow over the cavity under low- and high-backpressure conditions. The instantaneous planar measurements are analyzed to determine the mean and rms velocities in the streamwise direction. Under low-backpressure conditions, the velocity drop across the oblique shock attached to the cavity's leading edge is evident, while the modification of the mean and rms velocities is shown under high–backpressure conditions. These measurements demonstrate the benefits of hydroxyl tagging in comparison to particle based

methods that have difficulty in recirculation regions around high speed core flows. Future work will explore, in detail, approaches to making measurements in reacting cavities with high-speed cross flows.

Acknowledgements

References

1. Adrian, R. J., "Particle imaging techniques for experimental fluid mechanics," Annu. Rev. Fluid Mech., **23**, 261-304 (1991).
2. Drain, L. E., *The Laser Doppler Technique*, (Wiley, New York, 1980).
3. Maurice, M. S., "Laser velocimetry seed particles within compressible, vertical flows," AIAA J. **30**, 376-383 (1992).
4. Santoro, R. J., Pal, S., Woodward, R. D., Schaaf, L., "Rocket testing at university facilities," *39th AIAA Aerospace Sciences Meeting and Exhibit*, Paper No. 0748 (2001).
5. Marinelli, W.J., Kessler, W.J., Allen, M.G., Davis, S.J., and Arepalli, S. (1991) "Copper atom based measurements of velocity in turbulence and in arc jet flows," AIAA Paper 91-0358, 29th AIAA Aerospace Sciences Meeting and Exhibit, Reno, NV.
6. Allen, M., Davis, S., Kessler, W., Legner, H., McManus, K., Mulhall, P., Parker, T., and Sonnenfroh, D. "Velocity field imaging in supersonic reacting flows near atmospheric pressure," AIAA J **32**, 1676-1682 (1994)
7. Klavuhn, K. G., Gauba, G., McDaniel, J.C. OH laser-induced fluorescence velocimetry technique for steady, high-speed, reacting flows. J. Propul. Power **10,** 787-797 (1994).
8. Paul, P.H., Lee, M.P., Hanson, R.K., "Molecular velocity imaging of supersonic flows using pulsed planar laser-induced fluorescence of NO," Opt. Lett. **14,** 417-419 (1989).
9. Zimmermann, M. and Miles, R.B., "Hypersonic-helium-flow-field measurements with the resonant Doppler velocimeter,"Appl. Phys. Lett. **37**, 885-887 (1980).
10. McDaniel, J.C., Hiller, B., and Hanson, R.K., "Simultaneous multiple-point velocity measurements using laser-induced iodine fluorescence," Opt. Lett. **8**, 51-53 (1983).
11. Houwing, A. F. P., Smith, D. R., Fox, J. S., Danehy, P. M. and Mudford, N. R., "Laminar boundary layer separation at a fin-body junction in a hypersonic flow," Shock Waves **11**, 31-42 (2001).
12. Seasholtz, R. G., Zupanc, F.J., Schneider, S. J., "Spectrally resolved Rayleigh scattering diagnostic for hydrogen-oxygen rocket plume studies," J. Propul. Power **8**, 935-942 (1992).
13. Miles, R.B., Lempert, W.R., "Quantitative flow visualization in unseeded flows," Annu. Rev. Fluid Mech. **29**, 285-326 (1997).
14. Lempert, W. R., Jiang, N., Sethuram, S., and Samimy, M., "Molecular tagging velocimetry measurements in supersonic microjets," AIAA J. **40**, 1065-1070 (2002).
15. Hiller, B., Booman, R. A., Hassa, C., and Hanson, R. K., "Velocity visualization in gas flows using laser-induced-fluorescence of biacetyl," *Rev. Sci. Instrum.* **55**, 1964-1967 (1984).
16. Stier, B. and Koochesfahani, N. M., "Molecular tagging velocimetry (MTV) measurements in gas phase flows," Exp. Fluids **26**, 297-304 (1999).
17. Danehy, P. M., O'Byrne, S., Houwing, A. F. P., Fox, J. S., and Smith, D. R., "Flow-tagging velocimetry for hypersonic flows using fluorescence of nitric oxide," AIAA J. **41**, 263-271 (2002).
18. Orlemann, C., Schulz, C., and Wolfrum, J., "NO-flow tagging by photodissociation of NO_2. A new approach for measuring small-scale flow structures," Chem. Phys. Lett. **307**, 15-20 (1999).
19. Barker, P., Thomas, A., Rubinsztein-Dunlop, H., Ljungberg, P., "Velocity measurements by flow tagging employing laser enhanced ionisation and laser induced fluorescence," Spectrochim, Acta B **50**, 1301-1310 (1995).

20. Rubinzstein-Dunlop H., Littleton, B., Barker, P., Ljungberg, P., and Malmsten, Y., "Ionic Strontium fluorescence as a method of flow-tagging velocimetry," Exp. Fluids **30**, 36-42 (2001).
21. Krüger, S. and Grünefeld, G., "Stereoscopic flow-tagging velocimetry," Appl. Phys. B **69**, 509-512 (1999)
22. Ress, J. M., Laufer, G., and Krauss, R. H., "Laser ion time-of-flight velocity measurements using N_2^+ tracers," AIAA J. **33,** 296-301 (1995).
23. Pitz, R. W., Brown, T. M., Nandula, S. P., Skaggs, P. A., DeBarber, P. A., Brown, M. S., and Segall, J., "Unseeded velocity measurement by ozone tagging velocimetry," Opt. Lett. **21**, pp. 755-757 (1996).
24. Ribarov, L. A., Wehrmeyer, J. A., Batliwala, F., Pitz, R. W., and DeBarber, P. A. "Ozone tagging velocimetry using narrowband excimer lasers," AIAA Journal **37**, 708-714 (1999).
25. Pitz, R. W., Wehrmeyer, J. A., Ribarov, L. A., Oguss, D. A., Batliwala, F., DeBarber, P. A., Deusch, S., and Dimotakis, P. E., "Unseeded molecular flow tagging in cold and hot flows using ozone and hydroxyl tagging velocimetry," Meas. Sci. Tech. **11**, 1259 (2000).
26. Boedeker, L. R., "Velocity measurement by H_2O photolysis and laser-induced fluorescence of OH," *Opt. Lett.* **14**, 473-475 (1989).
27. Davidson, D. F., Chang, A. Y., DiRosa, M. D., and Hanson, R. K., " Continuous Wave Laser Absorption Techniques for Gasdynamic Measurements in Supersonic Flows," *Appl. Opt.* **30**, 2598-2608 (1991).
28. Wehrmeyer, J. A., Ribarov, L. A., Oguss, and Pitz, R. W., "Flame flow tagging velocimetry with 193 nm H_2O photodissociation," *Appl. Opt.* **38**, 6912-6917 (1999).
29. Ribarov, L. A., Wehrmeyer, J. A., Pitz, R. W., and Yetter, R. A., "Hydroxyl tagging velocimetry (HTV) in experimental airflows," *App. Phys. B* **74**, pp. 175-183 (2002)
30. Ribarov, L. A., Wehrmeyer, J. A., Hu, S., and Pitz, R. W., "Multiline hydroxyl tagging velocimetry measurements in reacting and nonreacting experimental flows," Experiments in Fluids, **37**, 65-74 (2004).
31. Dam, N. J., Klein-Douwel, J. H., Sijtsema, N. M., and ter Meulen, J. J., "Nitric oxide flow tagging in unseeded air," Optics Letters **26**, 36-38 (2001).
32. Sijtsema, N. M., Dam, N. J., Klein-Douwel, J. H., and ter Meulen, J. J., "Air photolysis and recombination tracking: A new molecular tagging velocimetry scheme," AIAA J. **40**, 1061-1064 (2002).
33. van der Laan, W. P. N., Tolboon, R. A. L., Dam, N. J., and ter Meulen, J. J., "Molecular tagging velocimetry in the wake of an object in supersonic flow," Exp. Fluid 3**4**, pp. 531-533 (2003).
34. Noullez, A., Wallace, G., Lempert, W. R., Miles, R. B., and Frisch, U., "Transverse velocity increments in turbulent flow using the RELIEF technique," J. Fluid Mech. **339**, 287-307. (1997).
35. Ben-Yakar, A. and Hanson, R. K. "Cavity flame-holders for ignition and flame stabilization in scramjets: an overview," J. Propul. Power **17**, 869-877 (2001).
36. Gruber, M. R. and Nejad, A. S., "New supersonic combustion research facility," J. Propul. Power **11**, 1080-1083 (1995).
37. Gruber, M. R., Baurle, R. A., Mathur, T., and Hsu, K.-Y. "Fundamental studies of cavity-based flameholder concepts for supersonic combustors," J. Propul. Power **17**, 146-153. (2001)
38. Gruber, M. R., Donbar, J. M., Carter, C. D., and Hsu, K.-Y., "Mixing and combustion studies using cavity-based flameholders in a supersonic flow," J. Propul. Power **20**, 769-778 (2004).
39. Rasmussen, C. C., Driscoll, J. F., Carter, C. D. and Hsu, K.-Y. „Characteristics of cavity-stabilized flames in a supersonic flow," J. Propul. Power 21, 765-768 (2005).
40. Pitz, R. W., Lahr, M.D., Douglas, Z. W., Wehrmeyer, J. A., Hu, S., Carter, C. D., Hsu, K. Y., Lum C., and Koochesfahani, M. M., "Hydroxyl tagging velocimetry in a supersonic flow over a cavity," Appl. Opt. **44**, 6692-6700 (2005).
41. Gendrich, C. P. and Koochesfahani, M. M., "A spatial correlation technique for estimating velocity fields using molecular tagging velocimetry (MTV)," Exp. in Fluids, **22**, 67-77 (1996).
42. Cohn, R. K. and Koochesfahani, M. M., "The accuracy of remapping irregularly spaced velocity data onto a regular grid and the computation of vorticity," Exp. in Fluids, **29(1)**, S61-S69 (2000).
43. Pitz R. W. and Daily, J. W. "Combustion in a turbulent mixing layer formed at a rearward-facing step," AIAA J., **21**, 1565-1570 (1983).
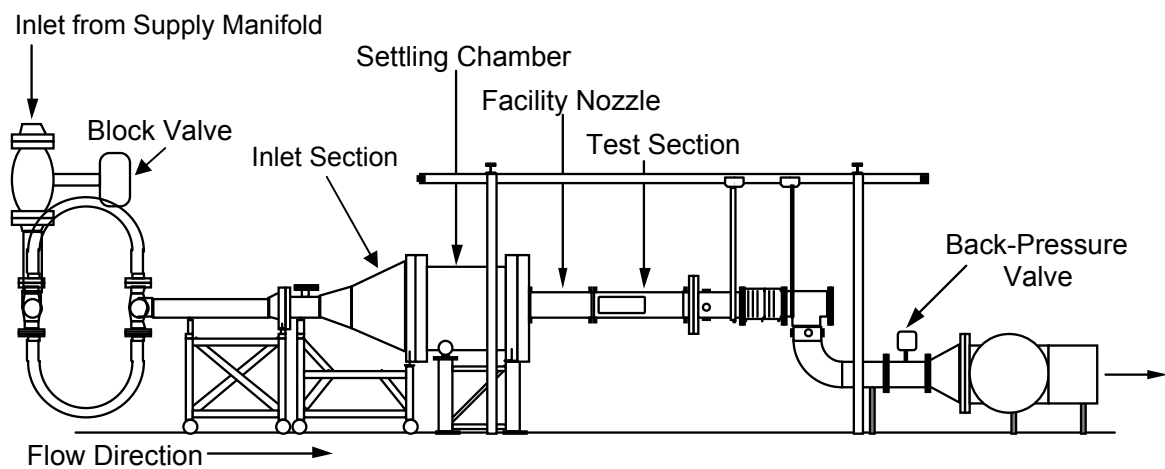
Fig. 1. Facility schematic of the supersonic combustion tunnel in Research Cell 19

American Institute of Aeronautics and Astronautics

Table 1. Mach 2 Flow with a Wall Cavity

Test	Stagnation Conditions		Isentropic Conditions Mach 2		Air Mass Flow Rate	Back Pressure Valve
	P_o	T_o	P	T		
	(kPa)	(K)	(kPa)	(K)	(kg/sec)	(%)
A	170	520	22	290	1.4	0
B	170	520	22	290	1.4	60
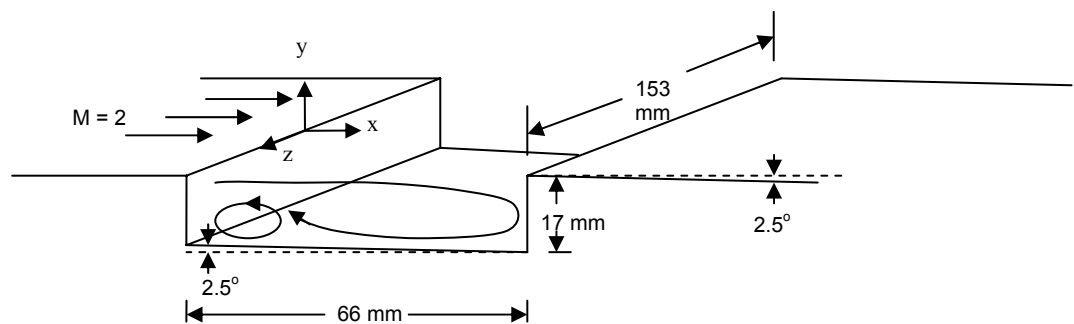
Fig. 2. Mach 2 Cavity Piloted Flow

ND: YAG pumped dye laser with frequency doubler, ~282 nm

HTV ICCD Camera (308 nm)

1000 mm f.l. pos. spherical lens

Test Section

150 mm f.l. neg. cylindrical lens

300 mm f.l. cylindrical lenslets

Mirror

300 mm f.l. cylindrical lens

M = 2

50/50 Beam splitter

ArF excimer laser ~ 193 nm
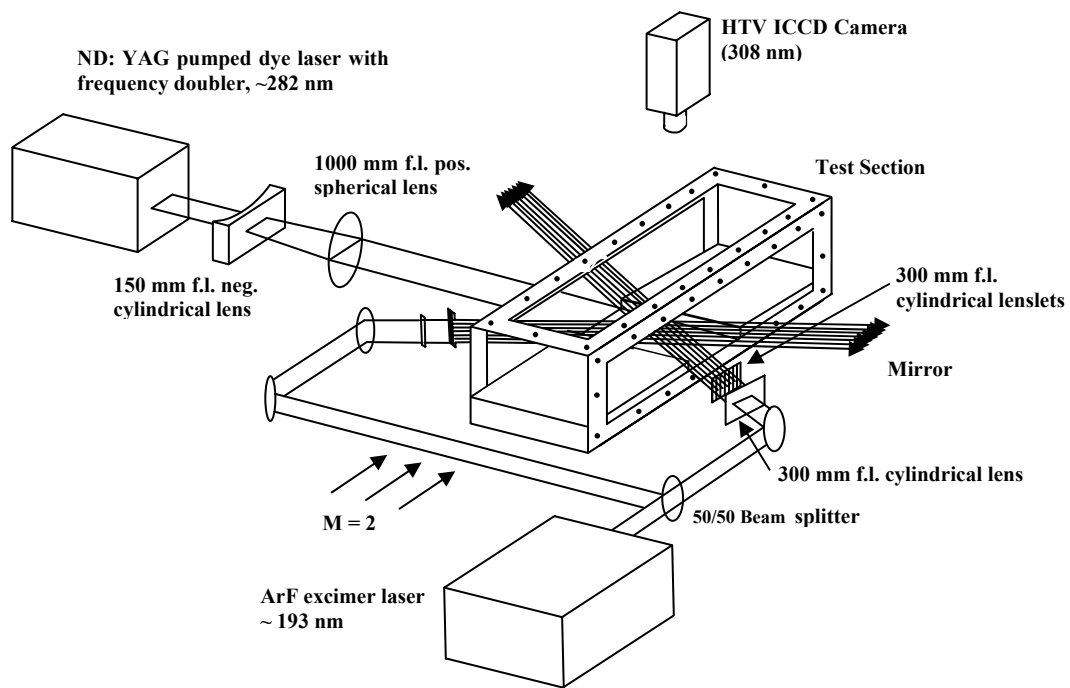
Fig. 3. Schematic of the HTV experimental system.

American Institute of Aeronautics and Astronautics
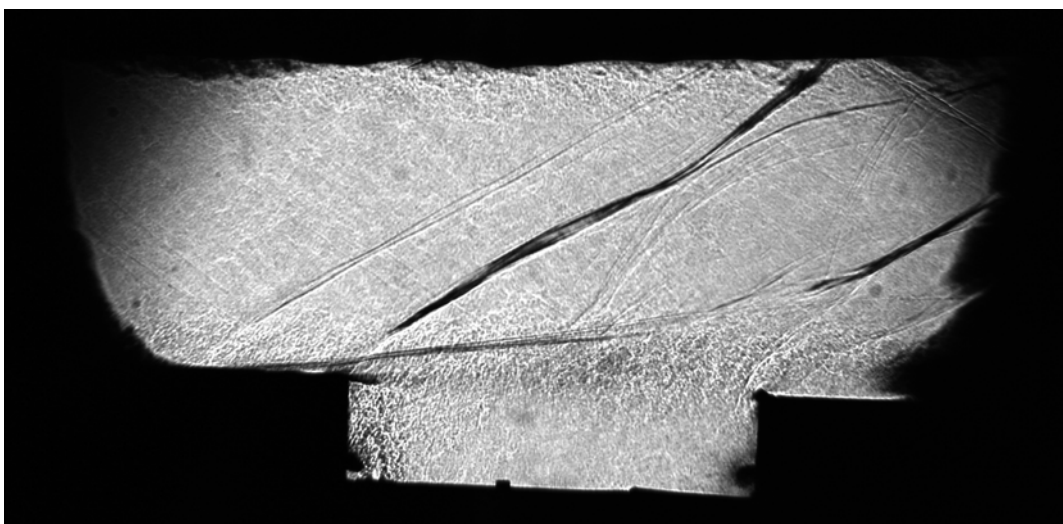
Fig. 4. Shadowgraph single-shot image over a rectangular cavity in a Mach 2 non-reacting cavity flow at low backpressure conditions.
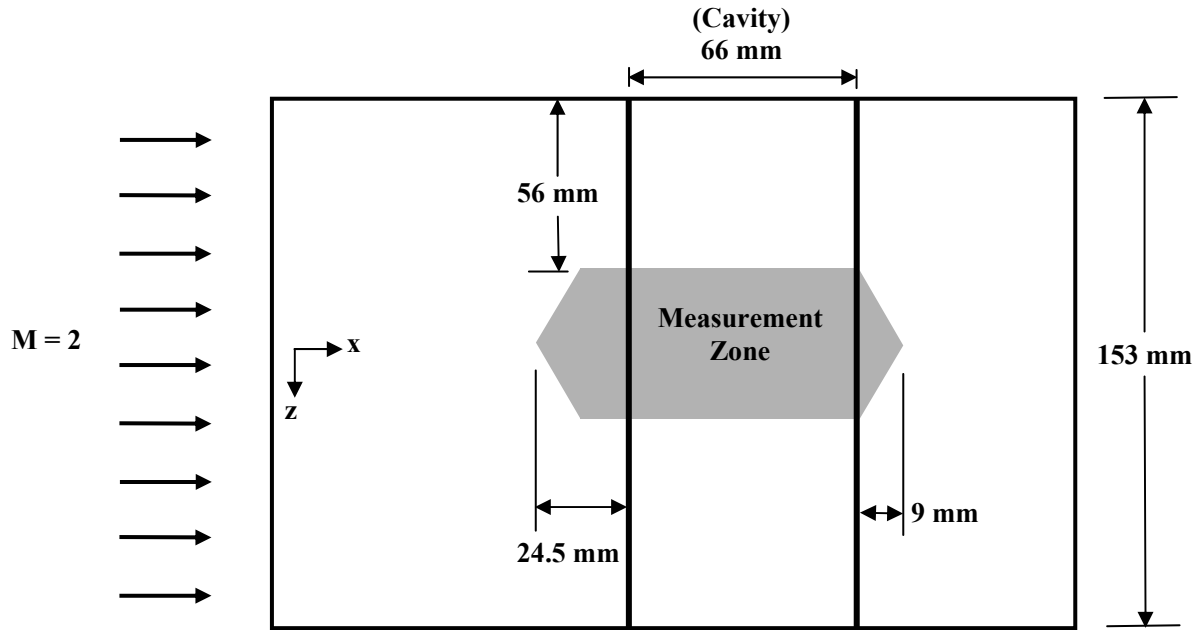
Fig. 5. Overhead schematic of the cavity, showing the position of the HTV images in regards to the cavity steps and test section walls.
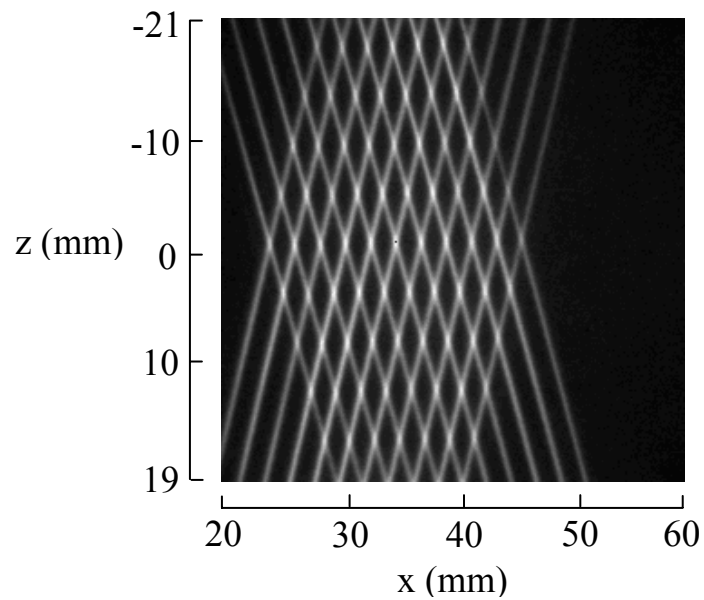
Fig. 6. Averaged un-delayed HTV image (at y = 15.62 mm, where z=0 is the centerline of the cavity and x=0 is at the front face of the cavity).
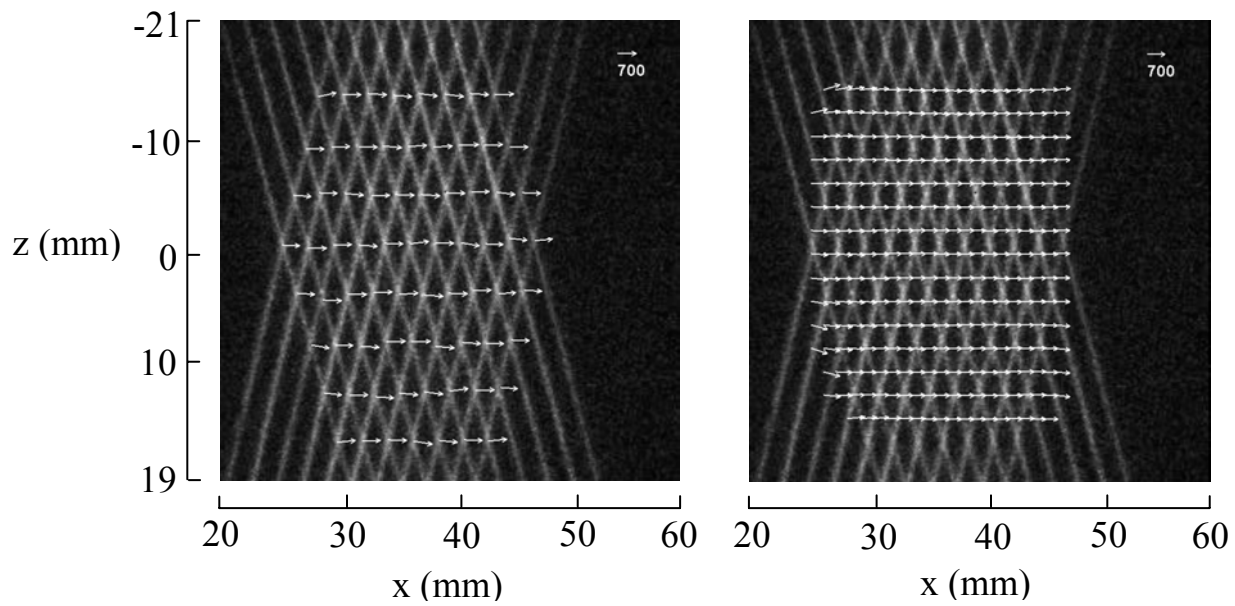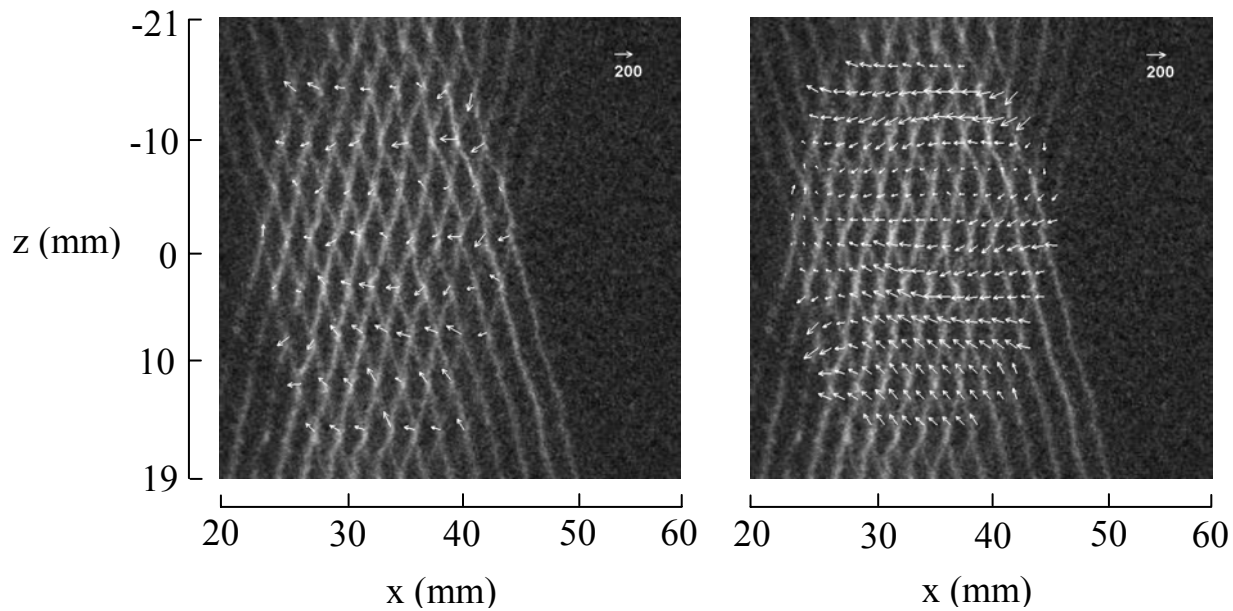
Fig. 7. Single-shot HTV images giving velocity images with an irregular (left) and regular grid (right) in a Mach 2 nonreacting scramjet cavity flow (at y = 15.62 mm, where z=0 is the centerline of the cavity and x=0 is at the front face of the cavity).
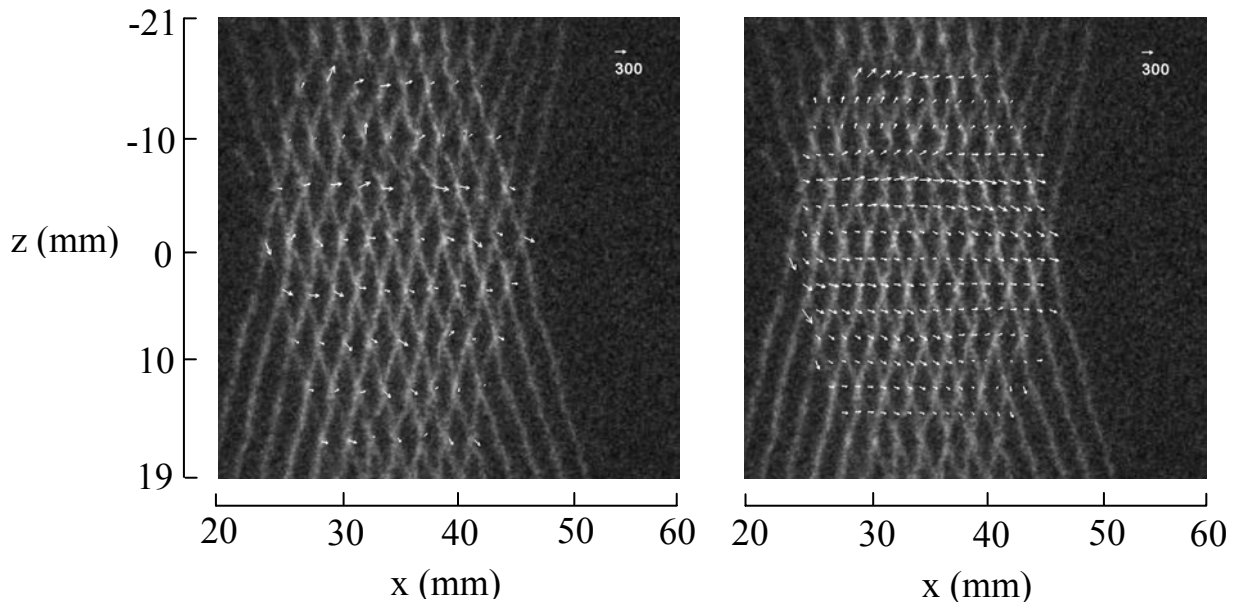
**Fig. 8. Single-shot HTV images giving velocity images with an irregular (left) and regular (right) grid in a Mach 2 nonreacting scramjet cavity flow (at y = .4064 mm, where z=0 is the centerline of the cavity and x=0 is at the front face of the cavity).**

Fig. 9. Single-shot HTV images giving velocity images with an irregular (left) and regular (right) grid in a Mach 2 nonreacting scramjet cavity flow (at y = -9.75 mm, where z=0 is the centerline of the cavity and x=0 is at the front face of the cavity).
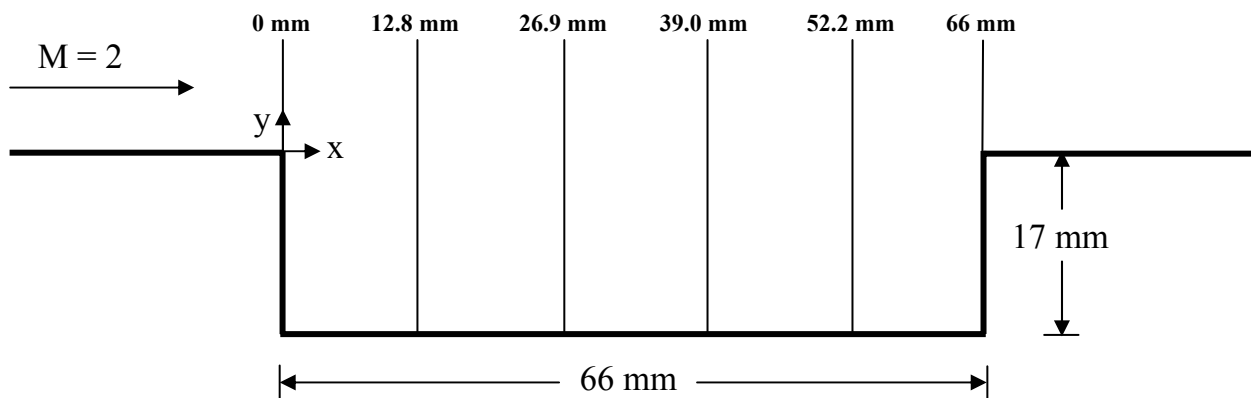
Fig. 10. Side-view schematic of the cavity, showing the profile locations along the x-axis.
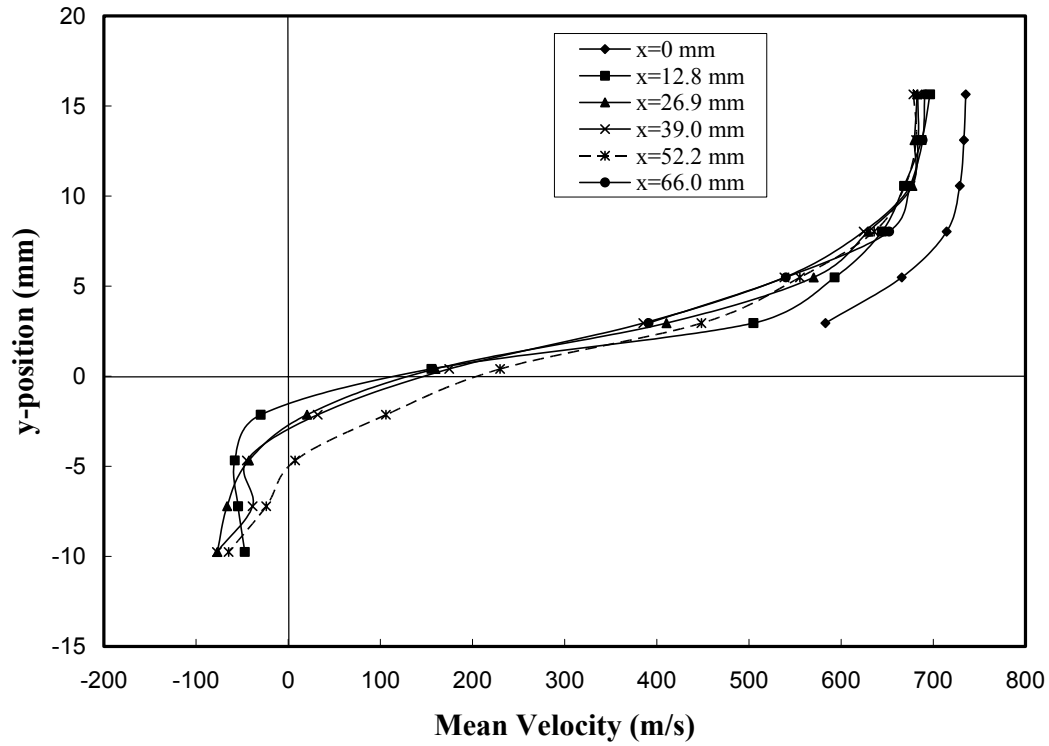
American Institute of Aeronautics and Astronautics

Fig. 11. Streamwise mean velocity profiles in the Mach 2 cavity flow showing shear layer between the freestream and the cavity at low backpressure conditions. (Near centerline, z = 0 mm where z=0 is the centerline of the cavity and x=0 is at the front face of the cavity)
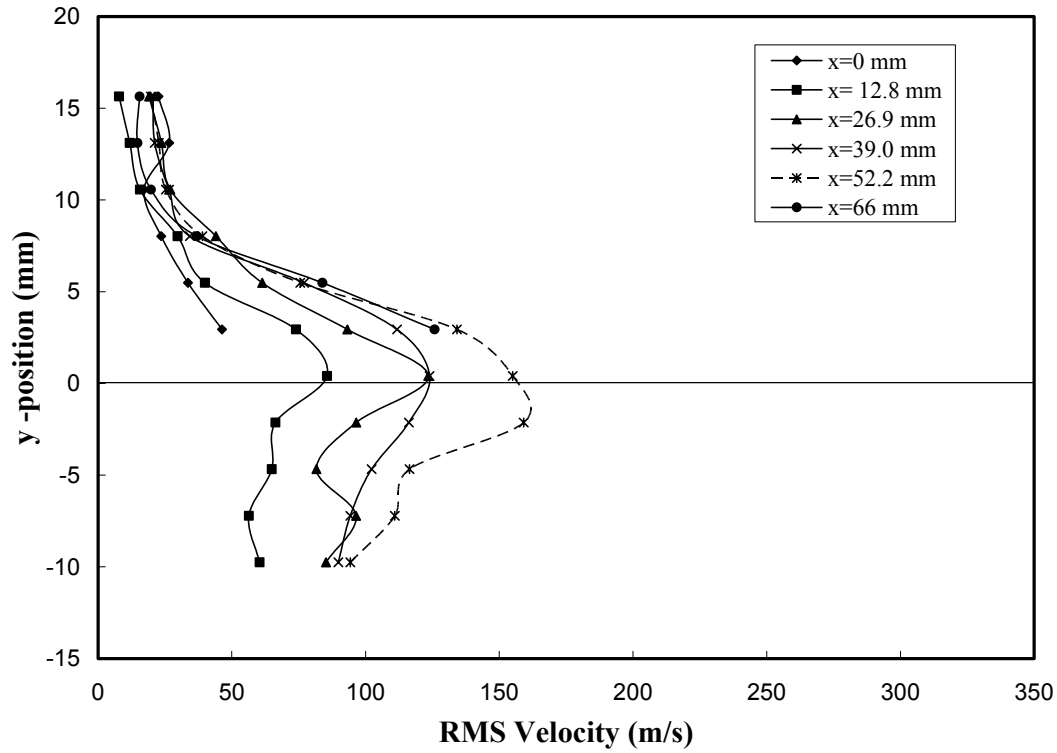

Fig. 12. Streamwise rms velocity profiles in the Mach 2 cavity flow showing shear layer between the freestream and the cavity at low backpressure conditions. (Near centerline, z = 0 mm where z=0 is the centerline of the cavity and x=0 is at the front face the cavity)
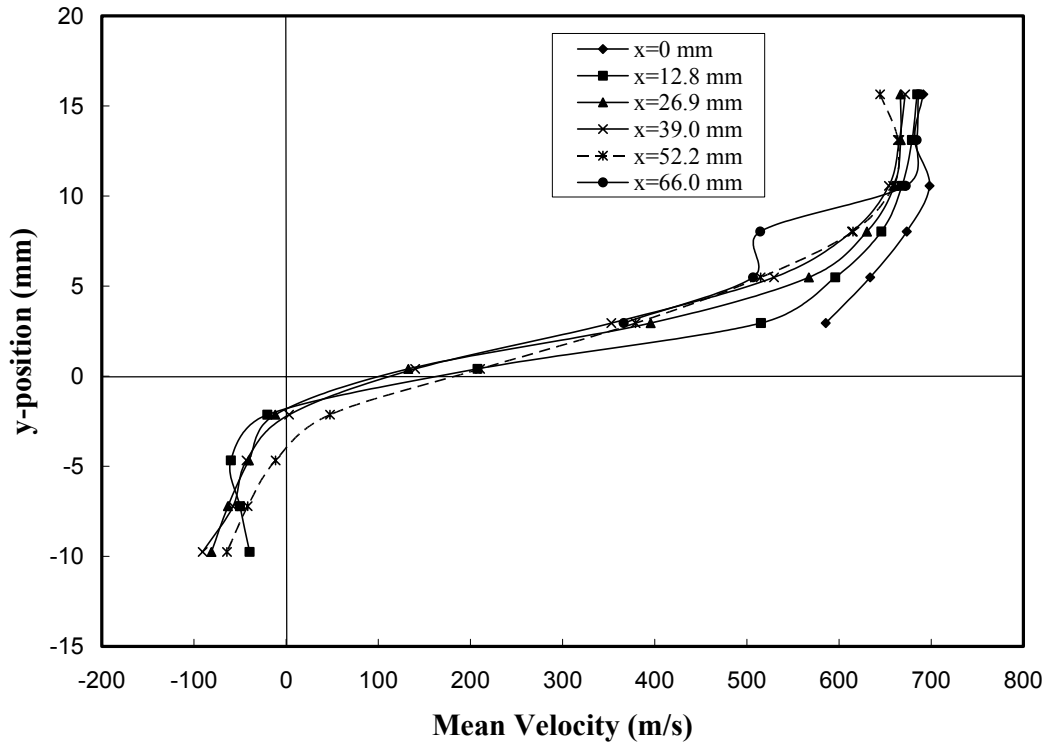
Fig. 13. Streamwise mean velocity profiles in the Mach 2 cavity flow showing shear layer between the freestream and the cavity at high backpressure conditions. (z = 0 mm where z=0 is the centerline of the cavity and x=0 is at the front face of the cavity)
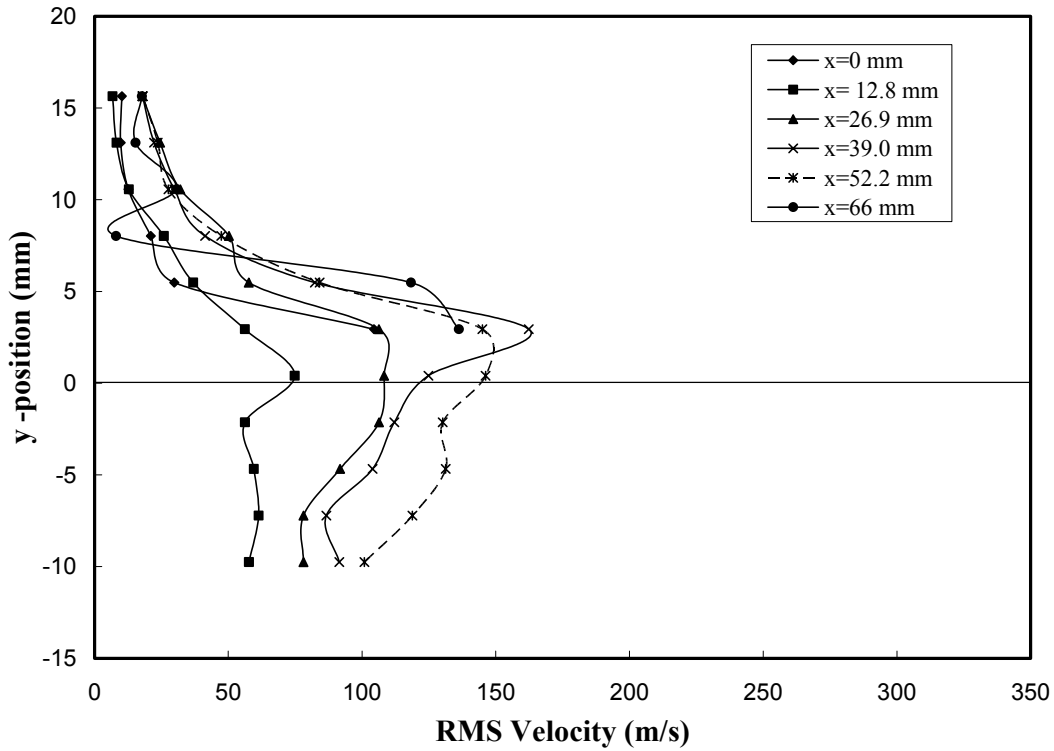

Fig. 14. Streamwise rms velocity profiles in the Mach 2 cavity flow showing shear layer between the freestream and the cavity under high backpressure conditions. (z = 0 mm where z=0 is the centerline of the cavity and x=0 is at the front face of the cavity)